A R C H I V E S O F M E T A L L U R G Y A N D M A T E R I A L S
Volume 57 2012 Issue 1
DOI: 10.2478/v10172-012-0015-6

A. CEGLAREK*, D. PŁUSA*, P. PAWLIK*, M. DOŚPIAŁ*

INFLUENCE OF HEAT TREATMENT ON MAGNETIC PROPERTIES OF NANOCRYSTALLINE $Nd_9Fe_{84}Zr_1B_6$ RIBBONS RECEIVED BY RAPID SOLIDIFICATION METHOD

WPŁYW OBRÓBKI TERMICZNEJ NA WŁASNOŚCI MAGNETYCZNE NANOKRYSTALICZNYCH TAŚM $Nd_9Fe_{84}Zr_1B_6$ WYTWARZANYCH METODĄ SZYBKIEGO CHŁODZENIA

The effect of the annealing on the phase composition and magnetic properties of nanocomposite melt-spun $Nd_9Fe_{84}Zr_1B_6$ ribbons has been investigated. From the X-ray diffraction studies confirmed be thermomagnetic curves measurements results that the microstructure of the material investigated is composed of a mixture of magnetically hard $Nd_2Fe_{14}B$ and soft α-Fe, Fe_3B nanosized grains. The small amount of undesirable $Nd_2Fe_{23}B_3$ metastable phase has been found which do not decompose at the highest annealing temperature. The hysteresis loop measurements certify that the ribbon annealed at 863K show the best coupling between the hard and soft magnetic phases and thus the highest coercivity of 0.38T. The grain sizes increase with increasing annealing temperature causing the coercivity to be decrease.

Keywords: nanocomposites, rapid solidification method, Nd-Fe-B alloys, hard magnetic materials, nanocrystalline magnets

Zbadano wpływ wygrzewania na skład fazowy i właściwości magnetyczne taśm nanokompozytowych $Nd_9Fe_{84}Zr_1B_6$ otrzymanych metodą szybkiego chłodzenia cieczy na wirującym miedzianym bębnie. Badania mikrostruktury potwierdzają zależności krzywych termomagnetycznych, z których wynika, że stop składa się z ziaren o rozmiarach nanometrycznych faz: magnetycznie miękkich α-Fe, Fe_3B oraz magnetycznie twardej $Nd_2Fe_{14}B$. Stwierdzono niewielką ilość niepożądanej metastabilnej fazy, która nie ulega rozkładowi przy najwyższej temperaturze wygrzewania. Pomiary pętli histerezy magnetycznej dla taśmy wygrzanej w temperaturze 863K świadczą o najsilniejszych oddziaływaniach pomiędzy fazami, twardą i miękką. Rozmiar ziaren wzrasta we wzrostem temperatury wygrzewania, powodując spadek koercji. Koercja taśmy wygrzanej w temperaturze 863K ma największą wartość, wynoszącą 0.38T oraz najmniejszy rozmiar ziarna fazy $Nd_2Fe_{14}B$.

1. Introduction

Nanocomposite magnets belong to the latest generation of neodymium magnets made from Nd-Fe-B alloys. These magnets are produced from alloys with lower Nd concentration compared to those of magnetically hard $Nd_2Fe_{14}B$ phase ($Nd_{11.8}Fe_{82.4}B_{5.9}$ %at.) responsible for high magnetic properties of such magnets. The nanocomposite magnets consist of uniformly distributed hard magnetic $Nd_2Fe_{14}B$ (high magnetocrystalline anisotropy energy) and soft α-Fe or Fe_3B (high saturation magnetization) fine exchange coupled grains. If the grain diameters of both the hard and the soft phase are less than 50 nm the exchange interactions occurring between grains prevents the soft α-Fe reversal leading to the remanence $\mu_0 M_R$ and maximum energy product $(BH)_{max}$ enhancement [1-4].

In spite of considerably lower amount of $Nd_2Fe_{14}B$ phase in nanocomposite magnets compared to these based on Nd-Fe-B alloys (e.g. neodymium sintered magnets have 85% by volume of $Nd_2Fe_{14}B$ phase) magnetic properties are comparable to ones of other magnets and manufacturing costs are lower. The starting material for nanocomposite magnets production is the powder obtained from ribbons prepared by rapid quenching of the liquid alloy on a rotating copper wheel (melt-spinning process). Depending on the wheel speed the nanocomposites may be obtained either directly from the melt during the melt-spinning process (lower wheel speed) or by the annealing the precursor amorphous alloy (higher wheel speed) at appropriate temperature in order to obtain optimum microstructure and magnetic properties. With the aim of preventing the unwanted grain growth

* CZĘSTOCHOWA UNIVERSITY OF TECHNOLOGY, INSTITUTE OF PHYSICS, 42-200 CZĘSTOCHOWA, 19 ARMII KRAJOWEJ AV., POLAND

during crystallization a small amount (1% at.) of other constituents, usually zirconium or niobium is added [5].

If the content of Nd is below the stoichiometric one the magnetically soft $Nd_2Fe_{23}B_3$ metastable phase crystallizes as intermediary phase which undesirably influences the magnetic properties. However, only a few papers mention about the existence of this phase [6-10].

If the temperature of annealing is high enough the metastable phase decomposes into α-Fe and $Nd_2Fe_{14}B$ phases and if the time of annealing is short as possible the increase in grain size of the phases forming the nanocomposite is minimized and does not considerably influences the ribbon magnetic properties especially the coercivity $\mu_0 H_C$.

In spite of a lot of works published so far on the nanocomposites they are still the subject of intense study.

The aim of this work was to examine the phase composition and magnetic properties of $Nd_9Fe_{84}Zr_1B_6$ nanocrystalline ribbons annealed at different temperatures.

2. Experimental details; material studied

Alloy ingots with composition of $Nd_9Fe_{84}Zr_1B_6$ were obtained from high purity elements using the arc melting in the protective argon atmosphere. In order to homogenize the samples they were melted several times. By rapid cooling the liquid alloy on a rotating wheel at the linear velocity of 35m/s the amorphous ribbons were obtained which then were annealed at temperatures between 823K and 983K for 5 minutes.

The phase composition was analysed using a Bruker D8 Advance X-ray diffractometer with CuK_α radiation.

The hysteresis loops were measured using the LakeShore vibration sample magnetometer at a magnetic field up to 2T.

Thermomagnetic curves $\mu_0 M(T)$ were measured using the Faraday's force magnetometer operating at a field of 0.87 T in the temperature range of 300K-850K with the heating rate of 10K/min. The Curie temperatures were estimated from the minima of the $d(\mu_0 M(T))/dT$ curves.

3. Results and discussion

Fig. 1 shows the X-ray diffractograms for the as-spun sample and those annealed at temperatures between 823K and 923K. The diffractogram for the as-spun ribbon has a wide diffraction halo which is characteristic of the amorphous alloy. Diffractograms for the sample annealed at 823K and 863K have diffraction peaks corresponding to α-Fe and $Nd_2Fe_{14}B$ phases with visible amorphous halo. As the annealing temperature increases to 923K the amorphous halo decreases and peaks from Fe_3B and $Nd_2Fe_{23}B_3$ phases are observed. The relative intensity of diffraction peaks corresponding to the $Nd_2Fe_{14}B$ phase increases with increasing the annealing temperature which means that the amount of $Nd_2Fe_{14}B$ increases. At the same time, the intensity of peak at $2\theta = 44.69$ corresponding to the α-Fe decreases with the increase in the annealing temperature At the highest annealing temperature the peaks from metastable $Nd_2Fe_{23}B_3$ phase are still seen which means that this phase does not completely decompose.

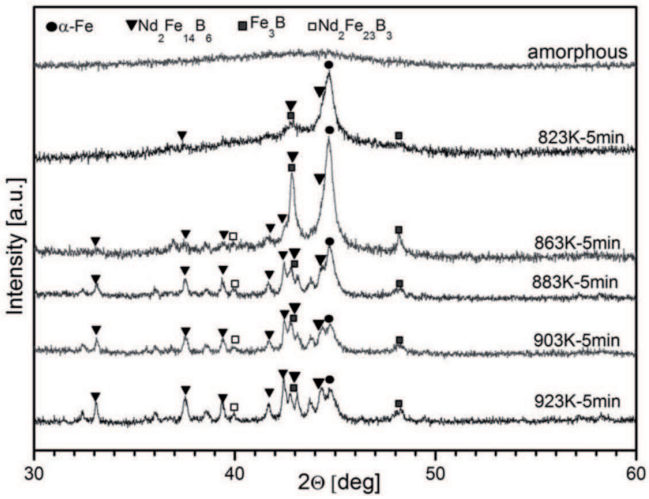

Fig. 1. X-ray diffractograms of $Nd_9Fe_{84}Zr_1B_6$ ribbons in the amorphous state and annealed at temperatures at the range of 823K-923K

From the diffraction lines broadening using the Scherrer's formula the average grain size of $Nd_2Fe_{14}B$ and α-Fe phases were estimated and listed in Tab.1. The smallest grain size of $Nd_2Fe_{14}B$ and α-Fe phases are equal to 50 nm and 28 nm, respectively for the ribbon annealed at 863K.

Crystallization of different phases influences the shape of the hysteresis loops as it is seen in Fig. 2 and 3.

From these loops the values of coervitity $\mu_0 H_C$, remanence $\mu_0 M_R$ and $(BH)_{max}$ were calculated. Hysteresis loops (for clarity reason the loops are presented in separated figures) in the second quadrant of coordinate system for the samples annealed at temperatures 883K (Fig. 2), 903K, 923K (Fig. 3) show a kink which is characteristic for the multi-phase samples. This is due to the lack of exchange interactions between the soft and hard phases which demagnetize independently showing the kink in the demagnetization curves [6]. Only for the sample annealed at 863K the demagnetization curve is smooth and shows no kink (Fig.2). Although there are some different phases the demagnetization curve for this sample shows a single-phase behaviour suggesting the

existence of the exchange interactions between the α-Fe, Fe_3B and $Nd_2Fe_{14}B$ grains [1-3].

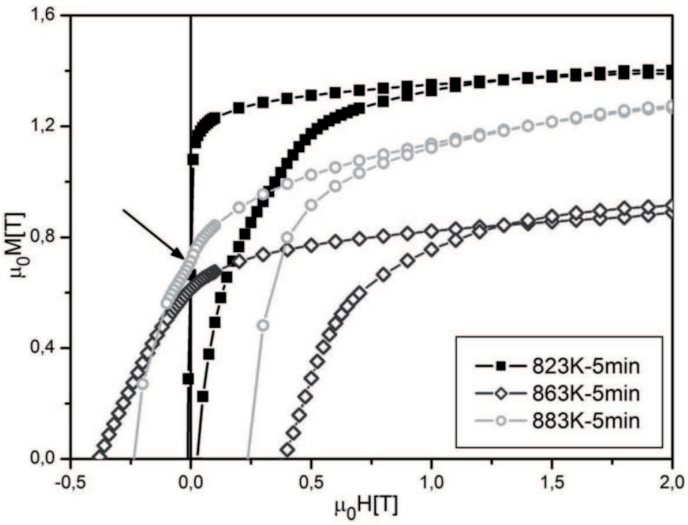

Fig. 2. Hysteresis loops of ribbons annealed at temperatures of 823K, 863K and 883K

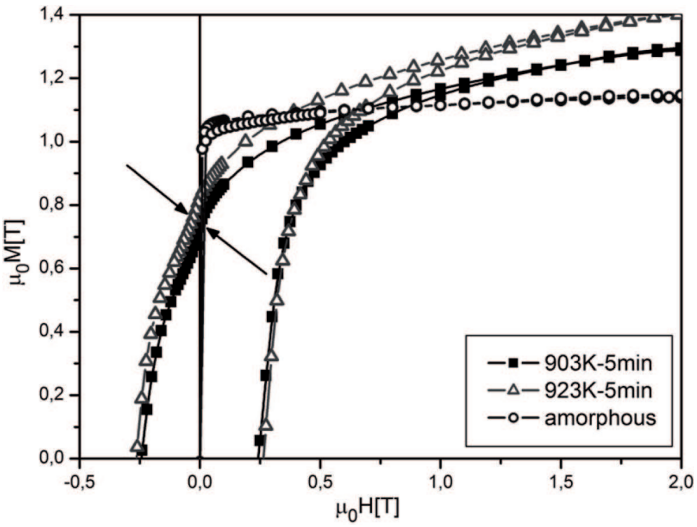

Fig. 3. Hysteresis loops for the amorphous as-spun ribbon and those annealed of 903K and 923K

The sample annealed at 863K has the largest value of coercivity, and the lowest remanence in spite of the existence of exchange interactions. This is likely due to the presence of certain amount of amorphous phase which lower the remanence. The decrease in the coercivity for higher annealing temperature is due to the increase in grain size (Table 1) whereas the increase the remanence as the annealing temperature increases is caused by the increasing amount of $Nd_2Fe_{14}B$ phase.

Fig. 4 presents the thermomagnetic curves M(T) for the samples annealed at 863K and 923K.

TABLE 1

Coercity $\mu_0 H_C$, remanence $\mu_0 M_R$, maximum energy product (BH_{max}) and grain size of ribbons at different annealing temperature

Annealing temperature [K]	$\mu_0 H_C$ [T]	$\mu_0 M_R$ [T]	The grain size of $Nd_2Fe_{14}B$ phase [nm]	The grain size of α-Fe phase [nm]	$(BH)_{max}$ [kJ/m^3]
823	0,24	0,69	-	36	2,2
863	0,38	0,61	50	38	34,1
883	0,23	0,71	121	64	36,7
903	0,25	0,75	131	70	35,7
923	0,26	0,82	222	73	45,4

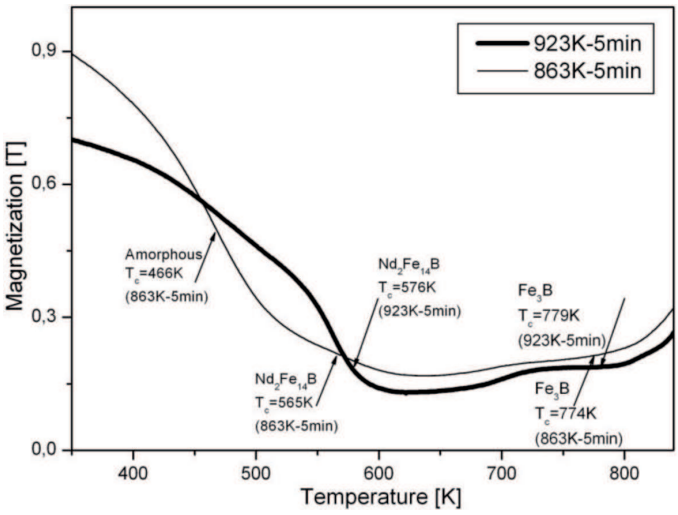

Fig. 4. Thermomagnetic curves for the ribbons annealed of 863K and 923K

The figure shows sudden falls in the magnetization curves caused by the phase transitions from the ferromagnetic to paramagnetic states confirming the multiphase structure of samples. The curves allow estimating the Curie temperature of phases present in the alloy. The values of the Curie temperature are presented in Tab.2 along with the data found in the literature [9, 11, 12]. The shape of the thermomagnetic curves shows that the metastable phase $Nd_2Fe_{23}B_3$ starts to decompose into the Fe_3B and α-Fe phases above 700K increasing the magnetization. Unfortunately, the highest possible temperature achieved in this experiment is too low to calculate the Curie temperature for α-Fe.

TABLE 2
The Curie temperature of the phases present in the alloy and found in the literature [9,11,12]

	T_c[K]	T_c[K][9]	T_c[K][11]	T_c[K][12]
Amorphous	466	–	–	463
$Nd_2Fe_{14}B$	576	583	585	573
$Nd_2Fe_{23}B_3$	–	658	655	–
Fe_3B	779	791	783	–

4. Conclusions

The method of obtaining samples allowed preparing nanocrystalline ribbons based on the $Nd_2Fe_{14}B$ phase doped with zirconium (1% at.).

Based on the research the following conclusions can be drawn:

- ribbons examined are multiphase, consisting of the magnetically hard phase $Nd_2Fe_{14}B$ and soft Fe_3B,α-Fe and $Nd_2Fe_{23}B_3$ phases
- the demagnetization curve is smooth for the ribbon annealed at the temperature of 863K, which signifies the existence of the exchange interactions between grains of α-Fe and $Nd_2Fe_{14}B$
- the grains size of α-Fe and $Nd_2Fe_{14}B$ increases with the increasing temperature causing the lower coercivity
- demagnetization curves of the ribbons annealed at higher temperature are characteristic for the multi-phase material.

REFERENCES

[1] E.F. Kneller, R. Hawig, IEEE Trans. Magn. **27** (4), 3588 (1991).

[2] R. Fischer, T. Schrefl, H. Kronmüller, J. Fidler, J.M.M.M. **150** 329-344 (1995).

[3] Y. Sen, S. Xiaoping, D. Youwei, Microelectronic Engineering **66**, 121-127 (2003).

[4] D. Płusa, M. Dośpiał, D. Derewnicka-Krawczyńska, P. Wieczorek, U. Kolarczyk, Arch. Metall. Mater. **56**, 151-153 (2011).

[5] B. Xiaoqian, Z. Jie, L. Wei, G. Xuexu, Z. Shouzeng, Journal of Rare Earths **27**, 843 (2009).

[6] A.M. Gabay, A.G. Popov, V.S. Gaviko, Ye.V. Belozerov, A.S. Yermolenko, J.Alloys Compd. **245**, 119 (1996).

[7] J. Park, D. Lee, T.Jang, Journal of Ceramic Processing Research **3**, 57 (2002).

[8] N. Talijan, T. Žák, J. Stajić-Trošić, V. Menushenkov, J.M.M.M. 258-259, 577 (2003).

[9] A. Jianu, M. Valeanu, D.P. Lazar, F. Lifei, M. Tomut, V. Pop, A. Alexandru, Romanian Reports in Physics **56**, 385 (2004).

[10] N. Talijan, J. Stajić-Trošić, A. Grujić, V. Ćosović, V. Menushenkov, R. Aleksić, J.Min.Met. **41B**, 85 (2005).

[11] M.V.P. Altoé, C.E. Echer, G. Thomas, Nanostructured Materials **8**, 19 (2007).

[12] S. Li, B. Gu, H. Bi, Z. Tian, G. Xie, Y. Zhu, Y. Du, J. Appl. Phys. **92**, 7514-7518 (2002).

Received: 10 January 2011.